Front. Mech. Eng. 2018, 13(2): 292–300
https://doi.org/10.1007/s11465-017-0443-0

RESEARCH ARTICLE

**Peng ZHOU, Zhike PENG, Shiqian CHEN, Yang YANG, Wenming ZHANG**

# Non-stationary signal analysis based on general parameterized time–frequency transform and its application in the feature extraction of a rotary machine



**Abstract** With the development of large rotary machines for faster and more integrated performance, the condition monitoring and fault diagnosis for them are becoming more challenging. Since the time-frequency (TF) pattern of the vibration signal from the rotary machine often contains condition information and fault feature, the methods based on TF analysis have been widely-used to solve these two problems in the industrial community. This article introduces an effective non-stationary signal analysis method based on the general parameterized time–frequency transform (GPTFT). The GPTFT is achieved by inserting a rotation operator and a shift operator in the short-time Fourier transform. This method can produce a high-concentrated TF pattern with a general kernel. A multi-component instantaneous frequency (IF) extraction method is proposed based on it. The estimation for the IF of every component is accomplished by defining a spectrum concentration index (SCI). Moreover, such an IF estimation process is iteratively operated until all the components are extracted. The tests on three simulation examples and a real vibration signal demonstrate the effectiveness and superiority of our method.

**Keywords** rotary machines, condition monitoring, fault diagnosis, GPTFT, SCI

## 1 Introduction

A safe and reliable running status of large rotary machines, such as generator sets, aircraft engines, and draught fans, plays an important role in industrial applications [1–6]. Therefore, the condition monitoring and fault diagnosis for these machines are significant. The operational process of a rotary machine contains speed raising and decline, load variation, and fault shutdown process. In these non-stationary processes, the instantaneous frequency (IF) of the vibration signal from the machine shows a nonlinear or a non-periodic changing rule, which implicates the rich information of the running condition of the machine [7]. If a fault occurs in these processes, then the fault feature will be reflected in the corresponding IF of the signal. Hence, the analysis for the IFs of these signals is one of the keys for condition monitoring and fault diagnosis.

Fourier transform is the most famous tool for frequency spectrum analysis. However, this tool cannot reveal the variance rule of the frequency with the time. To solve this problem, some effective time-frequency (TF) transforms were proposed, including the short-time Fourier transform (STFT), wavelet transform (WT), and Wigner-Ville distribution (WVD) [8]. However, these transforms have their own shortcomings, e.g., STFT lacks self-adaption, thereby producing the same scale in the whole TF plane. WT presents bad time resolution at a low frequency and bad frequency resolution at a high frequency, and WVD will generate a cross-term attributing to its bilinear structure. Furthermore, the common defect for the three methods is that they are non-parameterized.

Parameterized TF transforms have their own kernel functions. This kernel function determines the TF pattern that it fits to. Chirplet transform (CT) and Warblet transforms are two well-known deputies of the parameterized TF transforms [9–12]. The CT contains a quadratic polynomial kernel function. This kind of kernel function enables CT suitable to handle the linear frequency-modulated signal, whereas the Warblet transform contains a sine kernel function, which makes Warblet transform capable of processing the signal with a periodic TF pattern. However, the complex TF pattern, such as nonlinear or

Received November 28, 2016; accepted February 19, 2017

Peng ZHOU, Zhike PENG (✉), Shiqian CHEN, Yang YANG, Wenming ZHANG
School of Mechanical Engineering, Shanghai Jiao Tong University, Shanghai 201100, China
E-mail: z.peng@sjtu.edu.cn

non-periodic IF laws, will present one with bad resolution and concentration. Some modified versions exist for this issue, but these versions still cannot provide a general solution [8,13–15].

The general parameterized TF transform (GPTFT) was proposed to overcome the shortages of these classical TF analysis approaches [8]. The GPTFT is more than generalizing the classical parameterized TF analysis methods. The GPTFT reveals that the essence of the parameterized TF transform is based on a rotation and a shift operator with a kernel function, which maximizes the frequency resolution of the IF under "Heisenberg's uncertainty principle." The biggest merit of the GPTFT is its generalized kernel function. This method can adapt to the different kinds of TF patterns, whether linear or nonlinear, periodic or non-periodic. STFT, CT, Warblet transform, and FM$^m$ let transform [16] are special cases of the GPTFT.

The GPTFT are mainly focused on a mono-component or multi-component signals with the IFs of the same trend, because the GPTFT is only based on one kernel function [17]. However, circumstances occur with multi-component signals in reality, and the IFs of these components have different variation trends. The STFT and WT can also be used to deal with multi-component signals. However, their shortcomings will emerge again. EMD is one of the effective multi-component analysis methods, but this method is sensitive to noise and cannot process the situation with overlapped IFs [18,19]. Other multi-component analysis methods exist, but they may also be inappropriate in processing the case in this study [20–22]. For the GPTFT, we can use the rotation operator to estimate the IF of one component by defining a spectrum concentration index (SCI), although this method cannot be directly applied to handle the multi-component signal [17]. Then, the rotation operator with the estimated IF can be used to rotate the corresponding component to be stationary. This operation is a demodulation for the non-stationary signal. The stationary component in the TF plane can be filtered by a band-pass filter and reconstructed by multiplying the conjugation of the rotation operator. Finally, the reconstructed component can be subtracted from the multi-component signal. The IFs of the remaining components can be extracted through the same method. This process continues until all the components are extracted and such an extracting mode is often called greedy algorithm [17,23].

The remainder of this article is organized as follows. Section 2 introduces the definition of the GPTFT (its mathematical expression), kernel modeling, and the parameter identification method for the kernel. A simulation example based on the polynomial kernel is presented. Section 3 provides a general expression of the multi-component signal and the IF estimation process for the multi-component signal based on the SCI. The whole component extraction process is illustrated via a flow diagram. Two simulation examples are presented in this section. Section 4 verifies the practicability of the proposed IF extracting method through a real hydroturbine vibration signal. Section 5 concludes this article.

## 2 GPTFT

### 2.1 Definition of GPTFT

The corresponding analytical signal $z(t)$, which is generated by the Hilbert transform, $\boldsymbol{H}$, i.e., $z(t) = s(t) + j\boldsymbol{H}[s(t)]$, of any signal $s(t) \in L^2(R)$ is represented as follows:

$$z(t) = A(t)\mathrm{e}^{j2\pi\int IF(t)\mathrm{d}t}, \tag{1}$$

where $IF(t)$ is the IF of the signal $s(t)$. The GPTFT for $z(t)$ is defined as follows [8]:

$$TF_s(t_0,\omega;\mathbf{P}) = \int_{-\infty}^{+\infty} \bar{z}(t)\omega_\sigma^*(t-t_0)\mathrm{e}^{-j\omega t}\mathrm{d}t, \tag{2}$$

where

$$\begin{cases} \bar{z}(t) = z(t)\Phi_{\mathbf{P}}^{\mathrm{r}}(t)\Phi_{t_0,\mathbf{P}}^{\mathrm{s}}(t) \\ \Phi_{\mathbf{P}}^{\mathrm{r}}(t) = \mathrm{e}^{-j2\pi\int \kappa_{\mathbf{P}}(t)\mathrm{d}t} \\ \Phi_{t_0,\mathbf{P}}^{\mathrm{s}}(t) = \mathrm{e}^{j2\pi t\kappa_{\mathbf{P}}(t_0)} \\ \omega_\sigma(t) = \dfrac{1}{\sigma\sqrt{2\pi}}\mathrm{e}^{-\frac{t^2}{2\sigma^2}} \end{cases}.$$

In Eq. (2), $\Phi_{\mathbf{P}}^{\mathrm{r}}(t)$ and $\Phi_{t_0,\mathbf{P}}^{\mathrm{s}}(t)$ are kernel-based rotation and shift operator; $\kappa_{\mathbf{P}}(t)$ is an integrable kernel function, and $\mathbf{P}$ denotes its parameter set; and $\omega_\sigma(t)$ is the window function. The physical and geometrical meaning of these functions will be explained further.

The principle of the GPTFT is illustrated in Fig. 1 [8]. First, the IF of the signal is rotated by the rotation operator, $\Phi_{\mathbf{P}}^{\mathrm{r}}(t)$, which corresponds to that $IF(t)$ is subtracted by $\kappa_{\mathbf{P}}(t)$ at any time. Then, the rotated IF is shifted by the shift operator $\Phi_{t_0,\mathbf{P}}^{\mathrm{s}}(t)$ for $\kappa_{\mathbf{P}}(t_0)$. Finally, the STFT is operated by the window function, $\omega_\sigma(t)$. Evidently, no limitations exist for forming the kernel function, which guarantees the generality of the GPTFT. Moreover, the GPTFT will degrade the STFT, CT, and Warblet transform when $\kappa_{\mathbf{P}}(t) \equiv 0$, $\kappa_{\mathbf{P}}(t) = \alpha t$, and $\kappa_{\mathbf{P}}(t) = \beta\cos(\omega t)$, respectively.

Every part of the TF pattern of a signal has its own time and frequency resolution, such as the enclosed rectangle area, namely, the TF cell, in Fig. 1. The length and width of this area represent time and frequency resolution. The time resolution is only decided by the width of the window function, whereas the frequency resolution depends on the width of the window function and the slope of IF. Therefore, the frequency resolution of the IF after rotation

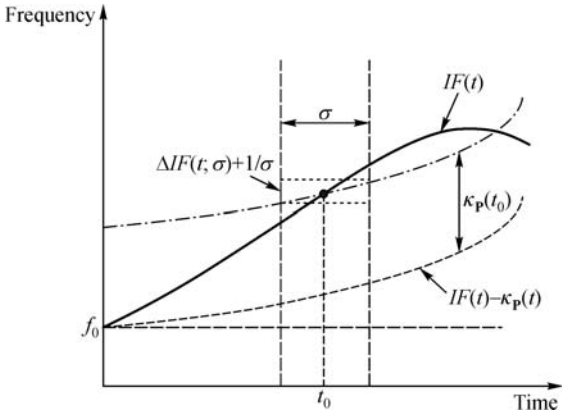


**Fig. 1** Principle of the GPTFT (vector graph)

and shift can be summarized as $\Delta IF(t;\sigma)+1/\sigma$ from Fig. 1. When the kernel function completely matches the IF of the signal, the slope of IF at every TF cell equals to zeros, i.e., $\Delta IF(t;\sigma)=0$. Thus, the frequency resolution reaches its minimum $1/\sigma$. Therefore, the GPTFT can provide a signal-dependent frequency resolution.

### 2.2 Kernel function modeling and parameter identification

According to the principle of the GPTFT above, the model of the kernel function and its parameter identification method are the keys for a satisfactory TF pattern of the GPTFT. Three frequently-used kernel models exist, namely, polynomial, Fourier series, and cubic spline. We focus on the polynomial kernel in this study [24]. And more detailed information for the other two models can refer to Refs. [8,12,25].

The GPTFT based on the polynomial kernel is called polynomial chirplet transform (PCT). It is a generalization of CT. The kernel function model of PCT is a general polynomial, which is embodied as follows:

$$\kappa_{\mathbf{P}}(t)=\sum_{i=2}^{n+1}\alpha_{i-1}t^{i-1}, \tag{3}$$

where parameter set $\mathbf{P}=\{\alpha_1,\alpha_2,...,\alpha_n\}$. Equation (3) is substituted into Eq. (2), and the rotation and shift operator can be embodied as follows:

$$\begin{cases}\Phi^{\mathrm{r}}_{\mathbf{P}}(\tau)=\mathrm{e}^{-j2\pi\sum_{i=2}^{n+1}\frac{\alpha_{i-1}t^i}{i}}\\ \Phi^{\mathrm{s}}_{t_0,\mathbf{P}}(\tau)=\mathrm{e}^{j2\pi\sum_{i=2}^{n+1}\alpha_{i-1}t_0^{i-1}t}\end{cases}. \tag{4}$$

We use the following nonlinear frequency modulated signal to demonstrate the superiority of the PCT compared with the classical TF transforms. The mathematic model of the signal is as follows:

$$s(t)=\cos\left[2\pi\left(30t-\frac{13t^2}{4}+\frac{1}{6}t^3\right)\right],\ 0<t<15\ \text{s}. \tag{5}$$

The IF of this signal is $IF(t)=30-6.5t+0.5t^2$. The sampling frequency is set at 100 Hz. This current signal is disturbed by a white Gaussian noise with a SNR of −3 dB. The TF patterns obtained by the STFT, WT, WVD, and PCT are illustrated in Fig. 2. The width of the window function for STFT and PCT is selected at 512 (default). The deficiencies discussed in the Introduction emerge in the TF patterns obtained by the STFT, WT, and WVD, but the PCT overcomes these deficiencies and provides an accurate and high-concentration TF pattern.

The parameter identification of the kernel function is achieved by an iterative peak-extracted algorithm with a rapid convergence speed. The detailed information of this algorithm can be found in Refs. [8,24]. The parameter identification result of IF for this example is presented in Table 1, which is near the real one ($f_1$ is the base frequency of the signal).

## 3 Multi-component IF extraction based on the GPTFT

### 3.1 SCI-based IF estimation method

The GPTFT is mainly focused on a mono-component signal or multi-component signals with the IFs of the same trend, because both require only one kernel function to match the IF. However, a number of situations occur with multi-component signals in reality, in which the TF patterns are completely different. The idea of the GPTFT can still be borrowed to solve this problem, although the IF extraction for the multi-component signal is much more complex than mono-component [17]. We start by defining the general multi-component frequency modulated signal to present a complete solution, as follows:

$$s(t)=\sum_{\kappa=1}^{m}a_\kappa(t)\cos\left[2\pi\left(f_\kappa t+\int\varphi_\kappa(t)\mathrm{d}t\right)\right]. \tag{6}$$

The IF of every component of the multi-component signal is $f_\kappa+\varphi_\kappa(t)$, where $f_\kappa$ denotes carrier frequency, and $\varphi_\kappa(t)$ denotes modulated one. In order to unify with the previous sections, Eq. (6) is taken Hilbert transform at first and the corresponding analytical signal is expressed as

$$\begin{aligned}z(t)&=s(t)+j\boldsymbol{H}\left(s(t)\right)\\&=\sum_{\kappa=1}^{m}a_\kappa(t)\mathrm{e}^{j2\pi\left(f_\kappa t+\int\varphi_\kappa(t)\mathrm{d}t\right)}.\end{aligned} \tag{7}$$

All the IFs are nearly impossible to extract at one time, because the TF pattern of each component may be absolutely different. Therefore, extracting them one by

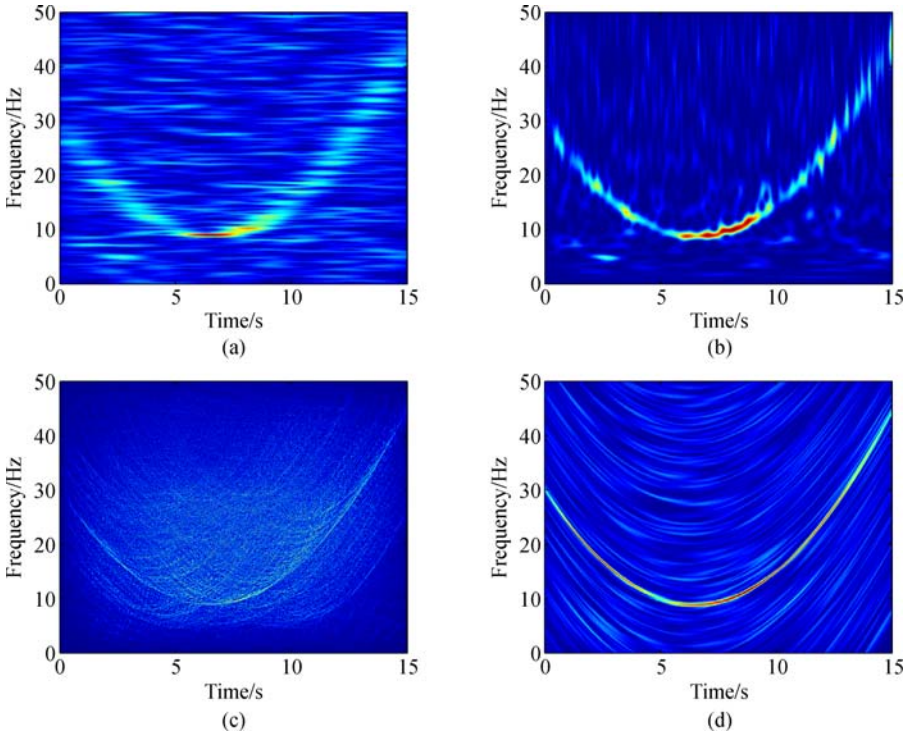


**Fig. 2** TF patterns of the signal in Eq. (5). (a) STFT; (b) WT; (c) WVD; (d) PCT

**Table 1** Estimated parameters based on the PCT for signal in Eq. (5)

| Parameter type | $f_1$ /Hz | $\alpha_1$ | $\alpha_2$ |
|---|---|---|---|
| Estimated | 29.898 | −6.446 | 0.492 |
| Exact | 30.000 | −6.500 | 0.500 |

one is a good substitute. Moreover, the rotation operator in the GPTFT can still be used to estimate the IF of one component by defining a SCI [17].

The multi-component model Eq. (7) multiplied by a rotation operator becomes the following:

$$\begin{aligned}\tilde{z}(t) &= z(t)\mathrm{e}^{-j2\pi\int\gamma(t;\mathbf{P})\mathrm{d}t} \\ &= \sum_{\kappa=1}^{m} a_\kappa(t)\mathrm{e}^{j2\pi\left(f_\kappa t+\int[\varphi_\kappa(t)-\gamma(t;\mathbf{P})]\mathrm{d}t\right)}.\end{aligned} \tag{8}$$

Then, the SCI can be applied to the Eq. (8) to evaluate the rotation effect

$$\mathrm{SCI}(\mathbf{P}) = E\left[|F(\tilde{z}(t))|^4\right], \tag{9}$$

where $F(*)$ stands for the Fourier transform, and $E(*)$ denotes the expectation on the frequency region. If the parameterized kernel function $\gamma(t;\mathbf{P})$ of the rotation operator completely matches the IF of a component in the signal, that one will be rotated as a stationary component at its carrier frequency. Actually, this is also a demodulation process. At that time, the frequency spectrum of the rotated signal would come into being a concentrated peak at the carrier frequency of the matched component. Also, the SCI reaches a local maximum on the parameter region $\mathbf{P}$ simultaneously. This phenomenon is the name source of SCI as depicted in Fig. 3 [17]. Hence, the SCI can be used to estimate the IF of every component in a multi-component signal with proper initial values of parameter set $\mathbf{P}$. The extraction sequence of IFs is ranked by the energy of every component of the signal follow-up to aim for an artificial process [17,23].

Based on the analysis above, every time the IF is extracted, the IF can transform to solve the following optimization problem:

$$\begin{aligned}\tilde{\mathbf{P}}_\kappa &= \arg\max_{\mathbf{P}} \mathrm{SCI}(\mathbf{P}) \\ &= \arg\max_{\mathbf{P}} E\left[|F\left(z(t)\mathrm{e}^{-j2\pi\int\gamma(t;\mathbf{P})\mathrm{d}t}\right)|^4\right].\end{aligned} \tag{10}$$

The kernel function of a rotation operator can be formulated by the polynomial, Fourier series, or the cubic spline according to Section 2.3. Hereinafter, the polynomial model and the corresponding PCT are employed to demonstrate the effectiveness of the proposed method. Thus, the kernel function $\gamma(t;\mathbf{P})$ and Eq. (10) can be

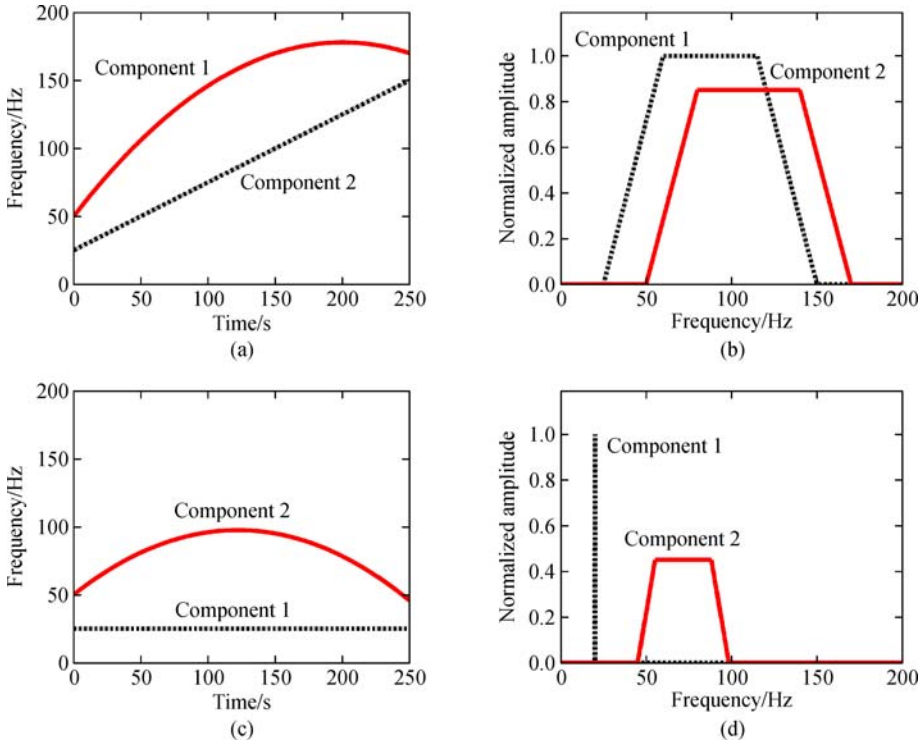


**Fig. 3** (a) TF pattern of the original signal; (b) frequency spectrum of the original signal; (c) TF pattern after rotation; (d) frequency spectrum after rotation

specified as follows:

$$\gamma(t;a_1,a_2,\ldots,a_n)=\sum_{i=1}^{n}a_i t^i, \tag{11}$$

$$\{\tilde{a}_1,\tilde{a}_2,\ldots,\tilde{a}_n\}_\kappa=\arg\max_{a_1,a_2,\ldots,a_n}\mathrm{SCI}(a_1,a_2,\ldots,a_n). \tag{12}$$

Equation (12) can be resolved by numerous optimization algorithms, and we select particle swarm optimization (PSO) in this article [17].

### 3.2 Multi-component IF extraction

When the IF of the component with the greatest energy has been estimated, a series of measures can be used to extract the corresponding component and continue this process. We present a flow diagram (Fig. 4) in this article to illustrate this extraction process, and a typical example is attached to explain this process. More detailed demonstration of this process can refer to Ref. [17].

Such an extracting mode ranked by energy is called greedy algorithm. An example to explain this algorithm is the following formula:

$$z(t)=z_1(t)+z_2(t)=\mathrm{e}^{j2\pi(10t+0.5t^2)}+\mathrm{e}^{-0.03t}\mathrm{e}^{j2\pi\left(20t+2t^2-\frac{t^3}{15}\right)},\ 0<t<15\ \mathrm{s}. \tag{13}$$

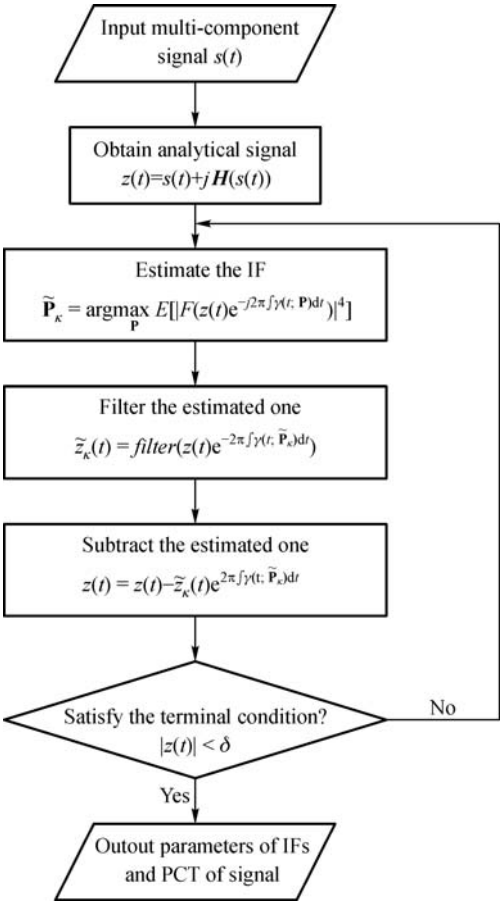


**Fig. 4** Multi-component IF extraction process (vector graph)

The IFs of these two components are $f_1(t) = 10 + t$ and $f_2 = 20 + 4t - 0.2t^2$. The sampling frequency is set at 100 Hz. Moreover, this signal is disturbed by a white Gauss noise with a SNR of −5 dB. The order of the kernel function is set at two, and the search ranges of $a_1$ and $a_2$ for the PSO are set at [−10, 10] in this Section.

The main steps of the extraction process for this example are presented in Fig. 5. The STFT of the original signal with a SNR of −5 dB is depicted in Fig. 5(a). The first component with highest energy is rotated as a stationary signal at its carrier frequency with the estimated parameters by Eq. (12), and the TF pattern is illustrated in Fig. 5(b). Then, the first component is filtered by a band-pass filter and is reconstructed by modulating with the conjugation of the operation operator. The TF pattern of the filtered part and the PCT of the reconstructed one are shown in Figs. 5(c) and 5(d), respectively, whereas Fig. 5(e) shows the PCT of the second component after reconstructing with the same operation. Finally, the TF patterns of these two components are assembled in Fig. 5(f). The parameter estimation results for the IFs of the two components are displayed in Table 2.

A more complex example is handled subsequently to further demonstrate the effectiveness of our method. This example is a three-component signal, and the IF of one component intersects with the other two. The mathematic model of this signal is expressed as follows:

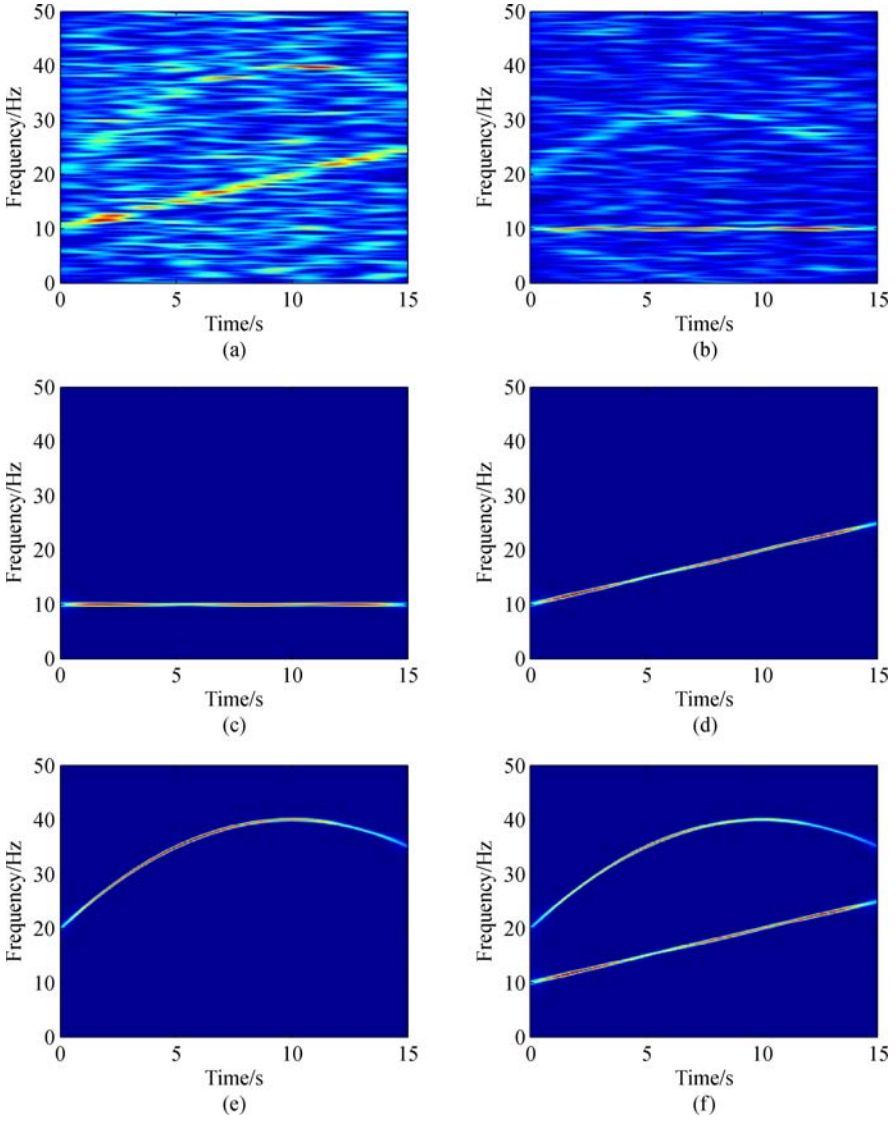


**Fig. 5** TF patterns in several steps of the proposed algorithm. (a) STFT of the original signal; (b) STFT after demodulating the first component; (c) filtering the first component; (d) PCT of the reconstructed component; (e) PCT of the second component; (f) assembled TF pattern

$$z(t) = z_1(t) + z_2(t) + z_3(t) = \mathrm{e}^{j2\pi\left(40t-\frac{7}{6}t^2\right)} + \mathrm{e}^{-0.05t}\mathrm{e}^{j2\pi\left(20t-\frac{2}{3}t^2+\frac{2}{45}t^3\right)} + 0.8\mathrm{e}^{-0.05t}\mathrm{e}^{j2\pi\left(5t+\frac{t^2}{3}\right)},\ 0<t<15\ \mathrm{s}. \quad (14)$$

The IFs of these three components are $f_1(t) = 40-\frac{7t}{3}$, $f_2 = 20-\frac{4t}{3}+\frac{2}{15}t^2$ and $f_3 = 5+\frac{2}{3}t$. The sampling frequency is set at 100 Hz. The current signal is disturbed by a white Gauss noise with a SNR of −5 dB.

For comparison, the STFT, WT, and WVD are also considered to present their results. In Fig. 6, the four TF patterns obtained by the STFT, WT, WVD, and our method are illustrated. The deficiencies concluded in the introduction to these three classical TF analysis methods become prominent for this complex signal. However, the TF pattern generated by our method exhibits a good anti-noise capability and resolution. The IFs of the three components are characterized accurately, and the parameters of the IFs identified by our method are listed in Table 3. The comparison with the real ones further demonstrates the effectiveness of this multi-component IF extraction method.

**Table 2** Estimated parameters based on the SCI for signal in Eq. (13)

| $k$ | Parameter type | $f_k$ /Hz | $a_1$ | $a_2$ |
|---|---|---|---|---|
| First one ($k$ = 1) | Estimated | 9.997 | 1.001 | $-1.159\times10^{-4}$ |
| | Exact | 10.000 | 1.000 | 0.000 |
| Second one ($k$ = 2) | Estimated | 20.001 | 3.998 | −0.199 |
| | Exact | 20.000 | 4.000 | −0.200 |

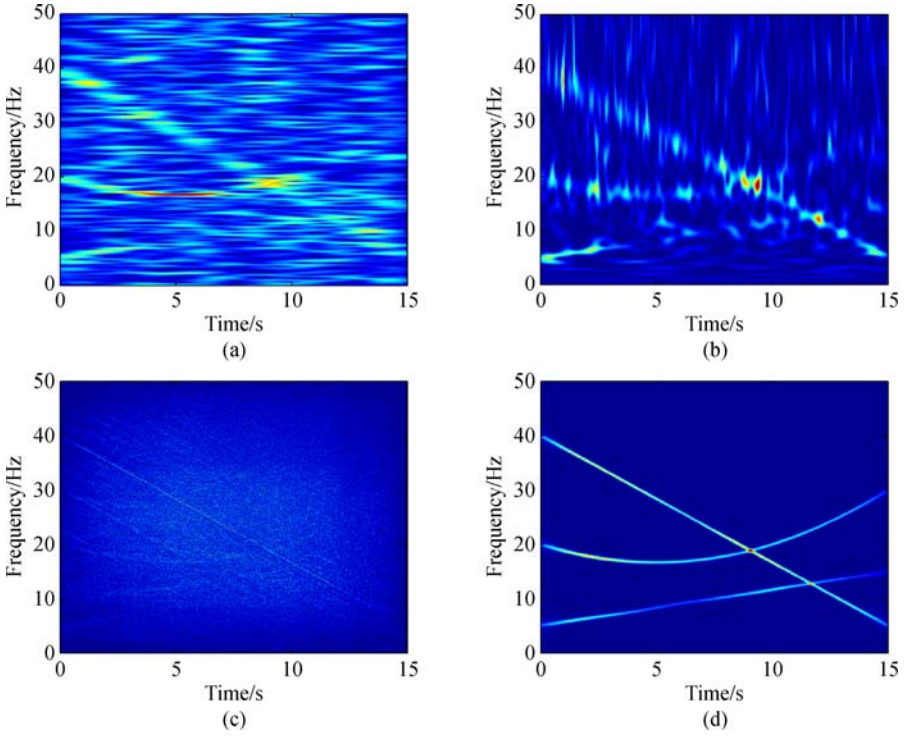


**Fig. 6** TF patterns of signal in Eq. (14). (a) STFT; (b) WT; (c) WVD; (d) assembled PCT

**Table 3** Estimated parameters based on SCI for signal in Eq. (14)

| $k$ | Parameter type | $f_k$ /Hz | $a_1$ | $a_2$ |
|---|---|---|---|---|
| First one ($k$ = 1) | Estimated | 39.995 | −2.332 | $-6.384\times10^{-5}$ |
| | Real | 40.000 | −7/3 | 0 |
| Second one ($k$ = 2) | Estimated | 19.998 | −1.331 | 0.133 |
| | Real | 20.000 | −4/3 | 2/15 |
| Third one ($k$ = 3) | Estimated | 4.996 | 0.663 | $5.150\times10^{-4}$ |
| | Real | 5.000 | 2/3 | 0 |

## 4 Application in feature extraction of a rotary machine

In this section, we use a real hydroturbine vibration signal to verify the practicability of our method [17,23]. This multi-component signal is measured from the shutdown process of a hydroturbine by the transducer. Moreover, the signal from this non-stationary process contains the fault information of the rotary machine. The sampling frequency is set at 16 Hz, and the sampled points are 1032. The width of the window function is set at 256. The order of kernel function is set at three, and the search ranges of $a_1$, $a_2$, and $a_3$ for the PSO are set at [–1, 1] in this section.

The STFT, WT, and WVD of the vibration signal are depicted in Figs. 7(a)–7(c), respectively. These methods fail to extract the TF features of the signal. The four components of this signal are successfully extracted one-by-one successfully. Due to the limited space, they are not exhibited individually but their assembled pattern is presented in Fig. 7(d). The estimated IF parameters of these components are presented in Table 4. Obviously, four components exist in this signal, which corresponds to the fundamental frequency component and the high-frequency ones (2×, 3×, and 4×). The TF features of these four components can be further used to compute the relevant physical quantities, such as the instantaneous speed of the rotator, and to achieve the condition monitoring and fault diagnosis ultimately [1–6].

## 5 Conclusions

This article discussed in detail an effective non-stationary signal analysis method based on the GPTFT. The definition and principle of the GPTFT were first introduced [8]. The kernel modeling and the parameter identification method for the GPTFT were illustrated. A typical example was used to present the superiority of the GPTFT over the classical TF transforms. Then, a multi-component IF extraction method was proposed based on the GPTFT [17]. The IF estimation of each component is the key step of this method. This step was accomplished by defining a

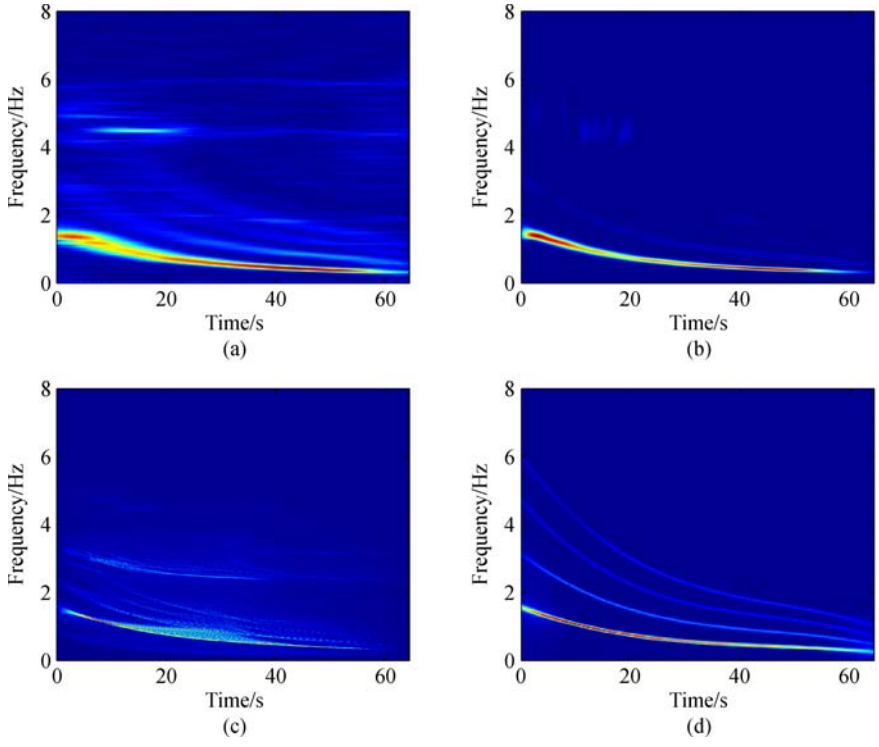


**Fig. 7** TF patterns of the hydroturbine vibration signal. (a) STFT; (b) WT; (c) WVD; (d) assembled PCT

**Table 4** Estimated parameters of the four IFs of the vibration signal

| Components | $f_k$ /Hz | $a_1$ | $a_2$ | $a_3$ |
|---|---|---|---|---|
| Fundamental frequency | 1.6045 | −0.0618 | 0.0011 | $-7.8561\times10^{-6}$ |
| 2× | 3.1383 | −0.1215 | 0.0023 | $-1.6728\times10^{-5}$ |
| 3× | 4.7132 | −0.1840 | 0.0036 | $-2.5872\times10^{-5}$ |
| 4× | 6.2118 | −0.2367 | 0.0045 | $-3.2075\times10^{-5}$ |

SCI. A greedy algorithm based on the GPTFT was executed subsequently until all the components had been extracted. The effectiveness of our method was demonstrated by two simulation signals and a real vibration signal, which implicates the potential of our method for feature extraction of the large rotary machine in order to achieve the condition monitoring and fault diagnosis [1–6].

**Acknowledgements** The authors gratefully acknowledge the support provided by the National Natural Science Foundation of China (Grant Nos. 11632011, 11472170, 51421092, and 11572189) to this work.

## References

1. Chu F, Peng Z, Feng Z, et al. Modern Signal Processing Approach in Machine Fault Diagnosis. Beijing: Science Press, 2009 (in Chinese)
2. Yang P. Data mining diagnosis system based on rough set theory for boilers in thermal power plants. Frontiers of Mechanical Engineering, 2006, 1(2): 162–167
3. Li W, Shi T, Yang S. An approach for mechanical fault classification based on generalized discriminant analysis. Frontiers of Mechanical Engineering, 2006, 1(3): 292–298
4. Chen X, Wu W, Wang H, et al. Distributed monitoring and diagnosis system for hydraulic system of construction machinery. Frontiers of Mechanical Engineering, 2010, 5(1): 106–110
5. Wang S, Chen T, Sun J. Design and realization of a remote monitoring and diagnosis and prediction system for large rotating machinery. Frontiers of Mechanical Engineering, 2010, 5(2): 165–170
6. Su H, Shi T, Chen F, et al. New method of fault diagnosis of rotating machinery based on distance of information entropy. Frontiers of Mechanical Engineering, 2011, 6(2): 249–253
7. Yang Y. Theory, methodology of parameterized time-frequency analysis and its application in engineering signal processing. Dissertation for the Doctoral Degree. Shanghai: Shanghai Jiao Tong University, 2013 (in Chinese)
8. Yang Y, Peng Z, Dong X, et al. General parameterized time-frequency transform. IEEE Transactions on Signal Processing, 2014, 62(11): 2751–2764
9. Mihovilovic D, Bracewell R. Adaptive chirplet representation of signals on time-frequency plane. Electronics Letters, 1991, 27(13): 1159–1161
10. Mann S, Haykin S. 'Chirplets' and 'warblets': Novel time-frequency methods. Electronics Letters, 1992, 28(2): 114–116
11. Angrisani L, D'Arco M, Schiano Lo Moriello R, et al. On the use of the warblet transform for instantaneous frequency estimation. IEEE Transactions on Instrumentation and Measurement, 2005, 54(4): 1374–1380
12. Yang Y, Peng Z, Meng G, et al. Characterize highly oscillating frequency modulation using generalized Warblet transform. Mechanical Systems and Signal Processing, 2012, 26: 128–140
13. Gribonval R. Fast matching pursuit with a multiscale dictionary of Gauss chirps. IEEE Transactions on Signal Processing, 2001, 49(5): 994–1001
14. Angrisani L, D'Arco M. A measurement method based on modificed version of the chirplet transform for instantaneous frequenct estimation. IEEE Transactions on Instrumentation and Measurement, 2002, 51(4): 704–711
15. Candès E J, Charlton P R, Helgason H. Detecting highly oscillatory signals by chiplet path pursuit. Applied and Computational Harmonic Analysis, 2008, 24(1): 14–40
16. Zou H, Dai Q, Wang R, et al. Parametric TFR via windowed exponential frequency modulated atoms. IEEE Signal Processing Letters, 2001, 8(5): 140–142
17. Yang Y, Peng Z, Dong X, et al. Application of parameterized time-frequency analysis on multicomponent frequency modulated signals. IEEE Transactions on Instrumentation and Measurement, 2014, 63(12): 3169–3180
18. Huang N, Shen Z, Long S, et al. The empirical mode decomposition and the Hilbert spectrum for nonlinear and non-stationary time series analysis. Proceedings of the Royal Society of London. Series A, 1998, 454(1971): 903–995
19. Wu Z, Huang N E. Ensemble empirical mode decomposition: A noise-assisted data analysis method. Advances in Adaptive Data Analysis, 2009, 1(1): 1–41
20. Mallat S G, Zhang Z. Matching pursuit in a time-frequency dictionary. IEEE Transactions on Signal Processing, 1993, 41(12): 3397–3415
21. Chen S S, Donoho D L, Saunders M A. Atomic decomposition by basis pursuit. SIAM Review, 2001, 43(1): 129–159
22. Dragomiretskiy K, Zosso D. Variational mode composition. IEEE Transactions on Signal Processing, 2014, 62(3): 531–544
23. Chen S, Yang Y, Wei K, et al. Time-varying frequency-modulated component extraction based on parameterized demodulation and singular value decomposition. IEEE Transactions on Instrumentation and Measurement, 2016, 65(2): 276–285
24. Peng Z, Meng G, Chu F, et al. Polynomial chirplet transform with application to instantaneous frequency estimation. IEEE Transactions on Instrumentation and Measurement, 2011, 60(9): 3222–3229
25. Yang Y, Peng Z, Meng G, et al. Spline-kernelled chirplet transform for the analysis of signals with time-varying frequency and its application. IEEE Transactions on Industrial Electronics, 2012, 59 (3): 1612–1621